Freeform Skeletal Shape Optimization of Compliant Mechanisms

Dong Xu

G. K. Ananthasuresh
e-mail: gksuresh@seas.upenn.edu

Department of Mechanical Engineering and Applied Mechanics,
University of Pennsylvania,
Philadelphia, PA 19104-6315

Compliant mechanisms are elastic continua used to transmit or transform force and motion mechanically. The topology optimization methods developed for compliant mechanisms also give the shape for a chosen parameterization of the design domain with a fixed mesh. However, in these methods, the shapes of the flexible segments in the resulting optimal solutions are restricted either by the type or the resolution of the design parameterization. This limitation is overcome in this paper by focusing on optimizing the skeletal shape of the compliant segments in a given topology. It is accomplished by identifying such segments in the topology and representing them using Bezier curves. The vertices of the Bezier control polygon are used to parameterize the shape-design space. Uniform parameter steps of the Bezier curves naturally enable adaptive finite element discretization of the segments as their shapes change. Practical constraints such as avoiding intersections with other segments, self-intersections, and restrictions on the available space and material, are incorporated into the formulation. A multi-criteria function from our prior work is used as the objective. Analytical sensitivity analysis for the objective and constraints is presented and is used in the numerical optimization. Examples are included to illustrate the shape optimization method. [DOI: 10.1115/1.1563634]

1 Introduction

Fully compliant mechanisms are elastic continua that are used to transmit or transform force and motion mechanically. The advantages of these mechanisms over rigid-body mechanisms are due to the absence of rigid-body kinematic joints. Some of the many advantages are less friction and wear [1], ease of manufacturing without assembly [2], provision for nonmechanical actuation [3], etc. Compliant mechanisms are used in product design (e.g., [4–7]), offshore structures [8], smart structures [9], Micro-Electro-Mechanical Systems [10], and minimally invasive surgery [11], etc. The systematic design of compliant mechanisms has received significant attention in the last decade resulting in two categories of methods. In the first category, rigid-body mechanism techniques are utilized [1,12,13] and in the second category structural optimization methods are suitably enhanced [14]. Since the subject matter of this paper is concerned with the latter category, a brief overview of those methods is provided below.

As in the design of any mechanical device, the first step in the design of compliant mechanisms is the generation of the concept where creativity and prior experience usually play a significant role. Since a fully compliant mechanism is a single entity of an elastic material continuum, the concept generation here entails the determination of the geometrical form of this continuum. Three levels of hierarchy are identified in the literature to describe the geometry: *topology*, *shape*, and *size*. Topology refers to the number of holes in the continuum and how different regions of interest (input/output ports and fixed portion) are connected to each other. Thus, a topology identifies a finite number of segments that are interconnected with each other. Once a topology is selected, the shapes of the individual segments need to be determined. The shape can either be the boundary shape of a 2-D or 3-D continuum or the skeletal shape of frame-like compliant mechanisms. The two types are schematically illustrated in Fig. 1. In boundary shape optimization, the shapes of the holes and/or the external boundary are varied. On the other hand, in skeletal shape optimization the shapes of the medial-axes of the segments are varied. The focus of this paper is on the skeletal shapes of individual compliant segments in a given topology. Finally, the size refers to the dimensions (thickness, width, etc.) that completely determine the physical form with a chosen topology and shape. The design methods developed for compliant mechanisms, although called the topology optimization methods, are capable of determining not only the topology but also the shape and size. However, there are some limitations to this approach as explained next.

1.1 Background and Motivation. The principal feature of the topology optimization methods is its design parameterization over a fixed reference design domain. Design parameterization refers to the set of variables that enable smooth variation of the geometrical form of the continuum and allow for large and significant variations in design. Smooth variation is necessary for gradient-based optimization methods. The phrase ''fixed reference domain'' implies that the geometric domain of interest is not altered during the iterative process of optimization. In the numerical implementation, when discretized finite element meshed-models are used, this simply means that the mesh is fixed implying that nodes are neither added/subtracted nor their connectivities and coordinates altered in any way. In this setting, variation of the geometrical form is accomplished in two ways. One is by altering the properties of a ''composite material'' composed of the actual material and void by way of the *homogenization method* [15] or simply by multiplying the material properties with a fictitious density function [16]. This is applicable when continuum finite elements, such as the plane-stress elements in the 2-D case, are used in the implementation. The other way is to assign a variable to each element in the mesh. If a *ground structure* of truss or frame elements is used, such a variable could simply be the thickness or the width of the rectangular cross-section. Both approaches have been adapted for compliant mechanisms. Ananthasuresh et al. [14], Sigmund [17], Nishiwaki et al. [18] and others have used the continuum elements; and Frecker et al. [19], Saxena and Ananthasuresh [20], and others have used the frame element-based ground structure approach. Figure 2 shows three examples solved using both the methods where, in addition to the topology, the shape and size are also determined simultaneously.

As can be seen in Fig. 2, in both methods, the shapes of the

Contributed by the Design Automation Committee for publication in the JOURNAL OF MECHANICAL DESIGN. Manuscript received July 2001; revised May 2002. Associate Editor: G. M. Fadel.

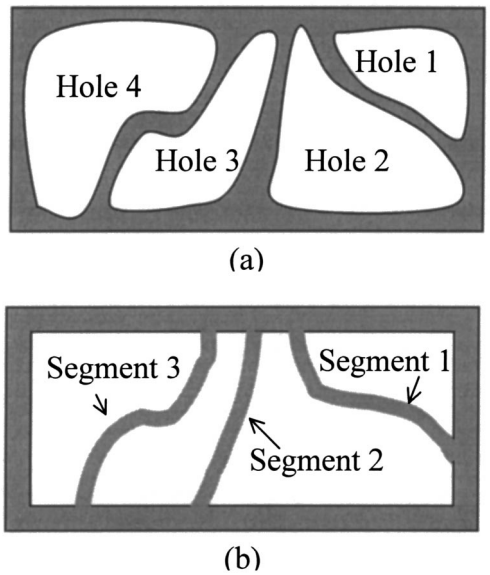

Fig. 1 Two types of shape optimization (*a*) optimizing the boundary shapes of holes (*b*) optimizing the skeletal curves of the segments. Both are capable of generating the same structure if the width of the segments is varied along with the curves in the latter.

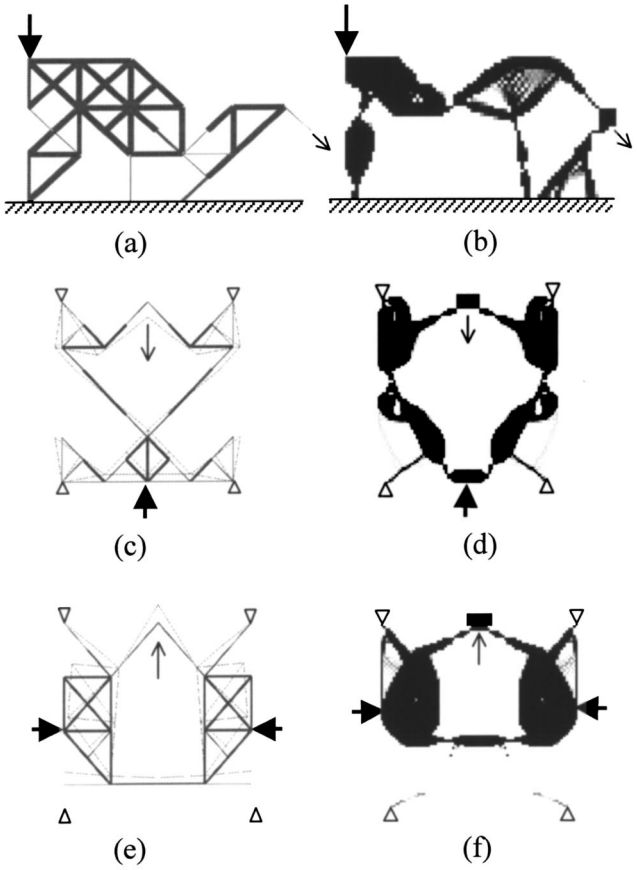

Fig. 2 Optimal topologies for compliant mechanisms using frame ground structure method (2*a*,2*c*,2*e*) and continuum element method (2*b*,2*d*,2*f*). The shapes of compliant segments in the ground structure designs have a limited number of slopes, and the continuum designs mostly rely upon flexural pivots.

flexible segments are restricted either by the type or the resolution of the design parameterization. If truss or frame elements are used (Figs. 2(*a*), 2(*c*), 2(*e*)), the shapes of the compliant segments are restricted to a finite number of slopes. If continuum elements are used (in this 2-D case, plane-stress elements) *flexural pivots* often appear (Figs. 2(*b*), 2(*d*), 2(*f*)). A flexural pivot is the location where two square plane-stress elements meet diagonally at a point or otherwise create a short and very thin segment connecting two relatively more rigid segments. In practice, this needs to be replaced with a longer flexural segment to avoid stress concentration and improve manufacturability [21]. Such flexural pivots do not take advantage of the distributed compliance (which is beneficial from the viewpoint of strength considerations) of a compliant segment. Furthermore, in order to obtain smooth shapes in either method, a very high resolution of the mesh is required. This increases the problem size. Thus, both methods are restrictive in terms of the shapes that they generate. To overcome this limitation, this paper focuses on optimizing the skeletal shape of the flexible segments in compliant mechanisms. This implies that a topology is necessary to begin the process of shape optimization. In this regard, the procedure outlined in this paper can be thought of as a second stage of optimization to further improve the performance of a compliant mechanism.

1.2 Organization of the Paper. In Section 2, related work on shape optimization of structures and compliant mechanisms is described. The statement of the shape optimization problem is outlined in Section 3 by presenting the design parameterization using Bezier curves, the objective function, and the constraints. Section 4 has sensitivity analysis and details of the solution procedure. Section 5 has two examples. The paper is concluded with some remarks in Section 6.

2 Related Work on Shape Optimization

There are different interpretations of shape optimization in the literature. For example, the procedure to obtain an optimum topological layout of a structure using frame elements has been called shape optimization of skeletal structures [22]. Most recent researchers focused on investigating the optimal shape of the boundaries of 2-D and 3-D structures. A lot of innovative methods have been investigated. A good review of shape optimization can be found in [23]. According to the object that is modified, the shape optimization methodology can be categorized as: entire domain based method that uses the finite element models; boundary surface based method that uses the boundary element method; and a boundary contour method. When a finite element model is used for shape optimization, it is necessary to discretize the whole design domain each time during the iterative process, while the boundary element-based method only requires the discretization of the boundary surface. The boundary contour method offers a further reduction in dimensions [24,25]. These are all gradient-based methods, where the function gradients are essential for the optimization techniques such as Sequential Quadratic Programming (SQP) method. On the other hand, techniques other than mathematical programming such as the genetic algorithms have also been applied to shape optimization. Some recent works on shape optimization that use genetic algorithms are described in [26] and [27].

From the perspective of the geometric model, or more specifically, the selection of the design variables, there are many approaches in the literature. Zienkiewicz and Campbell [28] defined the nodal coordinates of the finite element model as the design variables, which make the optimization task very difficult as arbitrary changes in the nodal coordinates could lead to improper topologies and shapes. In some other approaches, a set of key

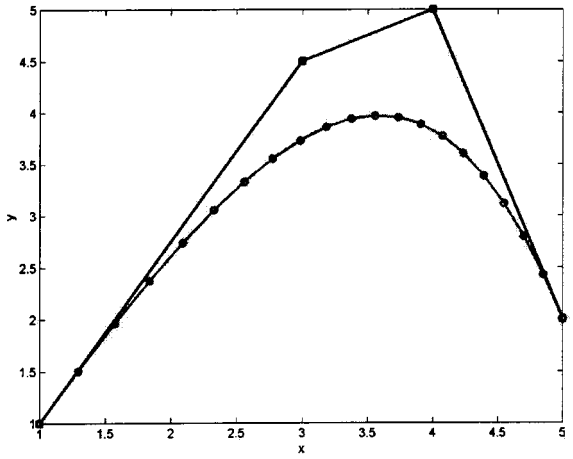

Fig. 3 Bezier control polygon and the corresponding curve

points or master nodes is used to define the geometry entities [29,30]. And recently the parametric and feature based CAD geometric modeling is becoming a powerful tool in shape optimization where some key dimensions are used to control the shape by describing the location of the control points. The connection between CAD and CAE makes it an easier task to carry out the FEA on the geometric model based on the CAD models.

In the compliant mechanisms literature, although there are numerous papers on topology optimization, the shape optimization has received very little attention. Hetrick and Kota [31] varied the coordinates of a few master nodes in a finite element model consisting of frame elements within a range in order to vary the shape. In the present paper, the shapes of the compliant segments in a given topology are allowed to vary freely in order to find the best *freeform* shape.

3 Problem Statement

The segment-wise, freeform shape optimization problem for compliant mechanisms is presented in this section. The design variables, the objective function, and the constraints are described in that order.

3.1 Design Parameterization. The primary criterion for choosing the design variables is that they cause smooth variations in the shape of a compliant segment. This will ensure that design derivatives can be easily computed for gradient-based optimization methods. The number of variables should be small enough but should be able to cover a large design space of shapes. *Bezier curves* satisfy both the requirements and are widely used in modeling curves. They are also simpler to use when compared to more sophisticated B-splines. A cubic Bezier curve in its parametric form is given by

$$\mathbf{P}(t)=[B_0(t) \quad B_1(t) \quad B_2(t) \quad B_3(t)] \quad [\mathbf{Q_0} \quad \mathbf{Q_1} \quad \mathbf{Q_2} \quad \mathbf{Q_3}]^T \tag{1}$$

where $\mathbf{P}(t)$ contains the x and y coordinates of a point on the curve corresponding to the parameter t which takes values from 0 to 1 from one end of the curve to the other end; B's are cubic Bernstein's basis functions given by

$$\left.\begin{aligned} B_0(t)&=(1-t)^3\\ B_1(t)&=3(1-t)^2t\\ B_2(t)&=3(1-t)t^2\\ B_3(t)&=t^3 \end{aligned}\right\} \tag{2}$$

and $\mathbf{Q}$'s are the x and y coordinates of four points that form the *Bezier control polygon*. Figure 3 shows the control polygon and the Bezier curve. By moving the control points, a wide variety of cubic curves that span a large design space of shapes can be obtained. It is then natural to use the coordinates of the control points as the design variables in shape optimization. One of the many interesting properties of the Bezier curves is that the curve always lies inside the convex hull of the control polygon. This is attractive from the viewpoint of applying constraints to restrict the curves to prescribed geometric domain. Another attractive property overcomes the need for re-meshing after every iteration, which is one of the main difficulties in most other shape optimization methods. This is because the points on the Bezier curve can be directly used as nodes in the finite element beam model. Furthermore, if uniform parameterization in t is used (i.e., from point to point, Δt is constant), the points on the curve are distributed such that more points (and therefore nodes) appear in the regions of large curvature. This can be explained as follows. The curvature c of a parametric curve P can be expressed as

$$c=\frac{|\dot{\mathbf{P}}\times\ddot{\mathbf{P}}|}{\dot{s}^3} \tag{3}$$

where $\dot{\mathbf{P}}$ and $\ddot{\mathbf{P}}$ are the first and second order derivatives of $\mathbf{P}$ with respect to the parameter t respectively (the cross product of them is a polynomial of parameter t), and $\dot{s}$ is the derivative of curve length with respect to the parameter t, i.e.,

$$\dot{s}\equiv\frac{ds}{dt}\approx\frac{\Delta s}{\Delta t} \tag{4}$$

Equations (3) and (4) indicate that the curvature is going to be larger when Δs is small for fixed Δt. In other words, for the region where the curvature is large, more nodes are going to be created which is desirable in a finite element model that uses two-noded beam elements. This is clearly evident in Fig. 3. Thus, an adaptive mesh is naturally created with uniform parameterization in t. Bezier curves are also amenable for analytical sensitivity analysis as explained later in Section 4.1.

3.2 Objective Function. Many objective criteria are used for the topology optimization of compliant mechanisms. The criteria used in [19] and [20] are used in this paper. The intent behind them is to achieve optimum balance between a flexibility measure and a stiffness measure because compliant mechanisms should be flexible enough to deform but a counter measure to prevent excessive, unbounded flexibility is also required. The mutual strain energy, MSE, is one criterion of flexibility as it is numerically equal to the output displacement. The strain energy, SE, is a measure of stiffness which is essentially the input displacement multiplied by the input force. Maximizing MSE makes the mechanism most flexible, and minimizing SE maximizes the stiffness. The two measures can be combined in several ways but only two are shown below.

$$\textit{minimize:-MSE/SE} \tag{5a}$$

$$\textit{minimize:-sign(MSE)}\frac{MSE^2}{SE} \tag{5b}$$

These objective functions are shown to possess unconstrained, non-unique, local minima in the topology optimization problem [20]. Such unconstrained minima are not likely to exist for the shape optimization problem, which as stated earlier, is a second-stage problem after the topology optimization stage. The shape optimization simply aims to improve upon the topology solutions by allowing for substantial shape changes that are not considered in the topology optimization. However, the existence of local unconstrained minima for shape optimization is also not completely ruled out. An example of this is illustrated in Fig. 5 for a compliant gripper shown in Fig. 4.

Figure 4(*a*) shows a polyethylene prototype of a compliant gripper while Fig. 4(*b*) is the schematic of the symmetric left half. The dark curve in Fig. 4(*b*) is the compliant segment whose shape is modified by varying the coordinates of the second and third points of the Bezier control polygon shown in dashed lines. Then MSE

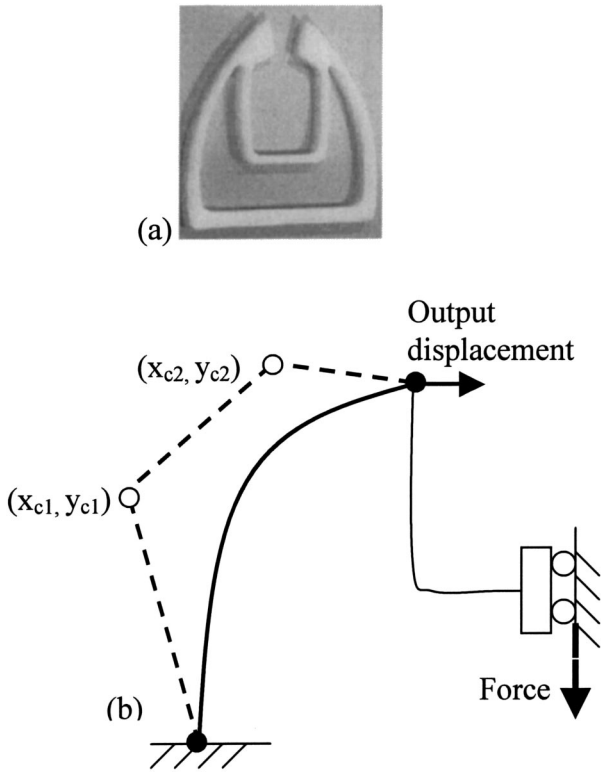

Fig. 4 (*a*) a compliant gripper (*b*) Schematic of the left half along with the Bezier polygon

and SE are both functions of x_{c1}, y_{c1}, x_{c2}, and y_{c2}. The objective functions in Eq. (5) are plotted in Fig. 5 where only one variable (y_{c2}) is varied. It can be seen that the second objective function possesses an unconstrained local minimum. It was also found to have an unconstrained minimum when both x and y coordinates of the second control point were varied [32]. Although such constrained minima could exist for shape optimization problems, some constraints cannot be avoided, and are in fact necessary to make the problem always well posed. In the presence of constraints, maximizing MSE itself can give good local constrained minima as shown in Section 5.

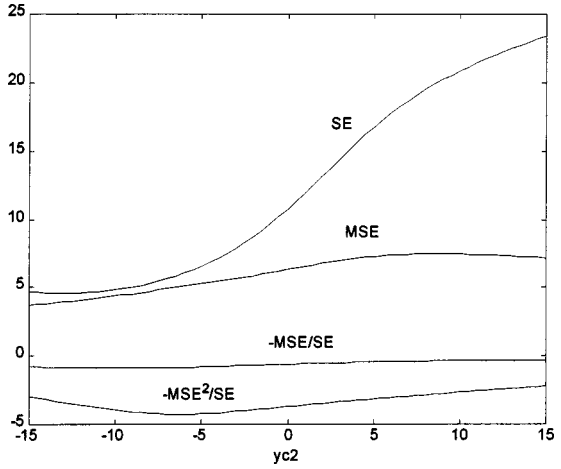

Fig. 5 Visualization of the objective functions by varying only one variable

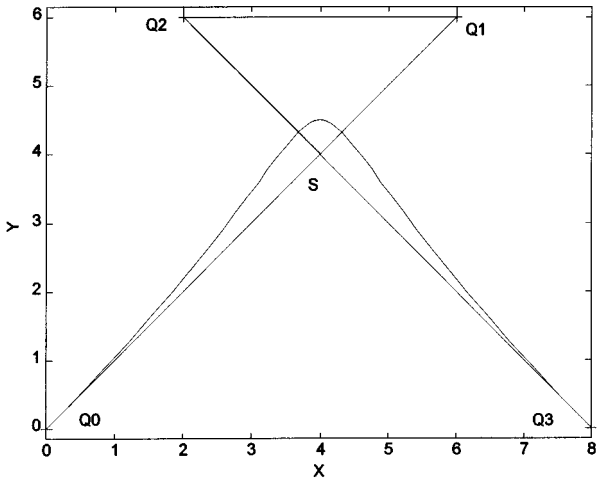

(a) $m = 1.5$, $n = 1.5$, $l.a.c. = -0.4167$

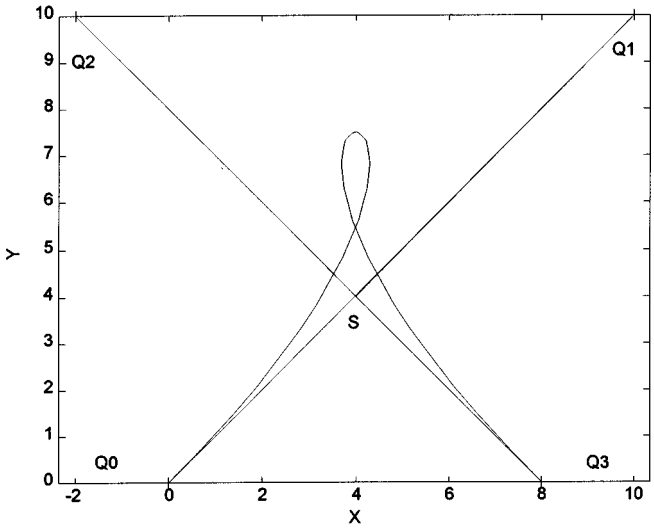

(b) $m = 2.5$, $n = 2.5$, $l.a.c. = 0.9167$

Fig. 6 Illustration of loop avoiding constraint (*a*) without a loop (*b*) with a loop

3.3 Constraints

Length Constraint. A constraint on the length of the compliant segment whose shape is optimized is often necessary in order to compare different shapes on the basis of a uniform measure. The length constraint also has economic implication in terms of material used. Formulating the length constraint is quite straightforward in the Bezier representation and in its beam element based finite element implementation used in this paper.

Loop-Avoiding Constraint. As the coordinates of the control polygon are varied, the Bezier curve can sometimes cross itself creating a loop. Such a loop is not meaningful when beam elements based finite element model is used, as it will not correspond to the physical model correctly. The constraint to avoid a loop can be formulated using the following condition [33]:

$$l.a.c. \equiv \left(m - \frac{4}{3}\right)\left(n - \frac{4}{3}\right) - \frac{4}{9} < 0 \tag{6}$$

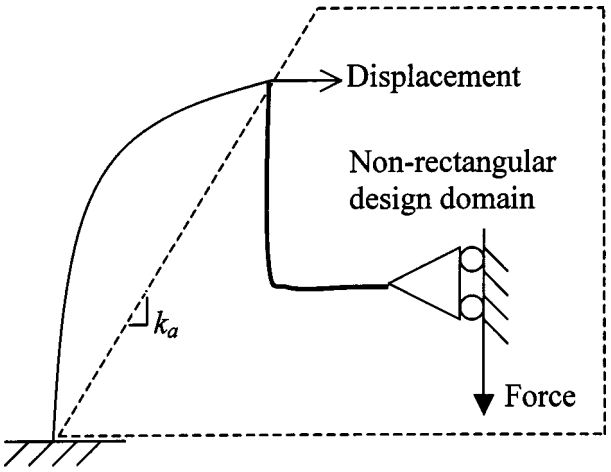

Fig. 7 Geometric constraints to prevent intersection of different segments. The permissible region for the control polygon of the segment in bold line is shown as a dashed line.

where m and n are given by

$$\mathbf{Q_1}-\mathbf{Q_0}=m(\mathbf{S}-\mathbf{Q_0})$$
$$\mathbf{Q_3}-\mathbf{Q_2}=n(\mathbf{Q_3}-\mathbf{S})$$

with **S** denoting the point of intersection of lines $\overline{\mathbf{Q_0Q_1}}$ and $\overline{\mathbf{Q_2Q_3}}$ in the Bezier control polygon. It is illustrated in Fig. 6 with two cases showing no loop ($l.a.c<0$) and a loop ($l.a.c.>0$) respectively. When $l.a.c.$ is zero, it indicates the occurrence of a cusp.

Intersection Avoiding Constraint. When two or more adjacent segments in a compliant topology are optimized, there is a danger of intersection among them. This can be easily dealt with because Bezier curves always lie within the convex hull of their corresponding control polygons. Therefore, by imposing geometric constraints on the nodal coordinates (design variables) of the designable control points, each segment can be restricted to desired region. Fig. 7 shows how one segment can be restricted to lie in a specified region. This introduces mostly linear constraints or lower and upper bounds on the design variables.

4 Implementation and Solution Procedure

First, one or more compliant segments are identified for shape optimization in a given topology. If the topology is obtained from a topology optimization method, compliant segments and rigid segments in it are identified. The experience with topology optimization indicates that they are almost always composed of flexible portions and relatively rigid segments [34]. These can be identified easily by examining the deformed profile of the solution. If a portion of the design displaces more or less like a rigid body rather than by elastic deformation, then it is a candidate for a rigid segment. A nominal shape is assigned to compliant segments that will be optimized for shape. Each compliant segment is then associated with a Bezier control polygon. In the examples presented in the next section, only the middle two control points are used to define design variables. The nodes for the beam elements are readily obtained by varying the parameter t uniformly from 0 to 1. As mentioned earlier, this enables re-meshing at no extra cost in addition to achieving appropriate node density in high and low curvature regions. Re-meshing here implies that the nodal coordinates are generated anew after every iteration. For the discretized two-noded, beam finite element model, the terms in Eq. 5 are given by

$$MSE=\mathbf{V}^T\mathbf{KU} \tag{7}$$

$$SE=\frac{1}{2}\mathbf{U}^T\mathbf{KU}$$

where **K** is the stiffness matrix of the entire compliant mechanism, **U** is the displacement vector under the applied input load **F** satisfying $\mathbf{KU}=\mathbf{F}$, and **V** is the displacement vector and the unit dummy load **f** applied at the output point and satisfying $\mathbf{KV}=\mathbf{f}$. The constraints are included as discussed in the previous section. MATLAB's ''constr'' function from the Optimization Toolbox, which uses the sequential quadratic programming algorithm, was used to solve the optimization problem. The derivatives were supplied to ''constr'' function using the sensitivity analysis described below.

4.1 Sensitivity Analysis. Considering one Bezier curve segment, the objective function in terms of the design variables, i.e., four coordinates of middle two control points is

$$f(x_{c1},y_{c1},x_{c2},y_{c2})=-MSE^2/SE \tag{8}$$

Since the objective function is indirectly related to the design variables via the coordinates of the control points, the nodal coordinates can be used as the bridge between the objective function and the design variables. The coordinates of nodes on the curve can be described in parametric form by substituting coordinates into Eq. (1) as shown below.

$$[x_k \quad y_k]=[B_0(t_k) \quad B_1(t_k) \quad B_2(t_k) \quad B_3(t_k)]\begin{bmatrix} x_0 & y_0 \\ x_{c1} & y_{c1} \\ x_{c2} & y_{c2} \\ x_3 & y_3 \end{bmatrix} \tag{9}$$

where the subscript k indicates the number of the node on the curve corresponding to the parameter t_k; x_0, y_0, x_3, y_3 are the coordinates of two end control points Q_0 and Q_3 respectively; x_{c1}, y_{c1}, x_{c2}, y_{c2} are the coordinates of two middle control points Q_1 and Q_2 respectively. By the chain rule of differentiation, the function gradients can be written as

$$\frac{\partial f}{\partial x_{c1}}=\sum_{k=1}^{NNODE}\frac{\partial f}{\partial x_k}\frac{\partial x_k}{\partial x_{c1}};\frac{\partial f}{\partial y_{c1}}=\sum_{k=1}^{NNODE}\frac{\partial f}{\partial y_k}\frac{\partial y_k}{\partial y_{c1}}$$
$$\frac{\partial f}{\partial x_{c2}}=\sum_{k=1}^{NNODE}\frac{\partial f}{\partial x_k}\frac{\partial x_k}{\partial x_{c2}};\frac{\partial f}{\partial y_{c2}}=\sum_{k=1}^{NNODE}\frac{\partial f}{\partial y_k}\frac{\partial y_k}{\partial y_{c2}} \tag{10}$$

The derivatives of the nodal coordinates with respect to the design variables are the Bernstein's basis functions as indicated below.

$$\frac{\partial x_k}{\partial x_{c1}}=B_1(t_k);\frac{\partial x_k}{\partial x_{c2}}=B_2(t_k)$$
$$\frac{\partial y_k}{\partial y_{c1}}=B_1(t_k);\frac{\partial y_k}{\partial y_{c2}}B_2(t_k) \tag{11}$$

The derivatives of the objective function with respect to the nodal coordinates are obtained using the normal procedure used in structural optimization [35]. For the sake of completeness, the derivatives of MSE and SE are given below.

$$\frac{\partial(MSE)}{\partial d_k}=-\mathbf{V}^T\frac{\partial\mathbf{K}}{\partial d_k}\mathbf{U} \tag{12a}$$

$$\frac{\partial(SE)}{\partial d_k}=\frac{1}{2}\mathbf{U}^T\frac{\partial\mathbf{K}}{\partial d_k}\mathbf{U} \tag{12b}$$

where d is any design variable. $\partial\mathbf{K}/\partial d_k$ in the above equations is obtained by assembling the element-wise derivatives, i.e., $\partial\mathbf{k}_{elem}/\partial d_k$ in the same manner as the global stiffness matrix **K** is assembled with $\mathbf{k}_{\text{elem}}$'s.

The sensitivities of the constraints are obtained in the same way. The length constraint and the loop-avoidance-constraint

given below, are nonlinear but can easily be dealt with through symbolic manipulation software such as MAPLE.

$$\sum_{n=1}^{NELEM} L_n = \sum_{n=1}^{NELEM} [(x_j - x_i)^2 + (y_j - y_i)^2]_n^{1/2} \leq L^* \quad (13a)$$

$$l.a.c. \equiv \left(m - \frac{4}{3}\right)\left(n - \frac{4}{3}\right) - \frac{4}{9} < 0 \quad (13b)$$

where

$$m = \frac{\sqrt{x_{c1}^2 - 2x_{c1}x_0 + x_0^2 + y_{c1}^2 - 2y_{c1}y_0 + y_0^2}}{\sqrt{\dfrac{(x_{c1}^2 - 2x_{c1}x_0 + x_0^2 + y_{c1}^2 - 2y_{c1}y_0 + y_0^2)(-x_0y_{c2} + x_0y_3 + x_3y_{c2} - x_{c2}y_3 - x_3y_0 + x_{c2}y_0)^2}{(-x_3y_{c1} + x_{c2}y_{c1} + x_3y_0 - x_{c2}y_0 + x_{c1}y_3 - x_0y_3 - x_{c1}y_{c2} + x_0y_{c2})^2}}}$$

$$n = \frac{\sqrt{x_3^2 - 2x_3x_{c2} + x_{c2}^2 + y_3^2 - 2y_3y_{c2} + y_{c2}^2}}{\sqrt{\dfrac{(x_3^2 - 2x_3x_{c2} + x_{c2}^2 + y_3^2 - 2y_3y_{c2} + y_{c2}^2)(x_{c1}y_3 + x_3y_0 - x_{c1}y_0 - x_0y_3 - x_3y_{c1} + x_0y_{c1})^2}{(-x_3y_{c1} + x_{c2}y_{c1} + x_3y_0 - x_{c2}y_0 + x_{c1}y_3 - x_0y_3 - x_{c1}y_{c2} + x_0y_{c2})^2}}}$$

In the examples solved, since there were more constraints than the design variables, direct method was used instead of the adjoint method [35].

5 Examples and Discussion

The compliant mechanism solutions obtained with topology optimization methods need to be studied carefully to extract a meaningful topology from them. One way to do this is through a kinematic interpretation of the mechanism solution. The question to ask here is the deformation of which segments is giving the required mobility to the mechanism. In the examples given in Fig. 2, such segments can easily be identified when undeformed and deformed configurations are superimposed on one another. Figure 2(*c*) and 2(*e*) show this where it can be seen which segments are critical for the functional character of the mechanism. In order to further improve the performance, shape optimization of such segments can be performed using the procedure outlined in this paper. Once the kinematic character of a topology understood, equivalent kinematic interpretation is often possible to simplify the topology and make it suitable for shape optimization. Similar interpretation is also possible with continuum topology solutions (Figs. 2(*b*), (*d*), and (*f*)) which often reply upon flexural pivots. The topologies considered in the two examples discussed in this section are equivalent kinematic interpretations of compliant topologies. These are chosen to illustrate the method over actual optimal compliant topologies because more constraints (segment intersection, for example) and practical considerations can be seen in these two examples.

5.1 Example1: Gripper. Taking the topology of the compliant gripper shown in Fig. 4(*a*), the following problem is posed for shape optimization. As shown in Fig. 8, only the left half is used due to symmetry. It is divided into two compliant segments that are represented as two Bezier curves. The end points of both the control polygons are fixed. This means that the fixed point, the output point, and the input point are not changed during shape optimization. The *x* and *y* coordinates of the middle control points on the left control polygon $(x_{b1}, y_{b1}, x_{b2}, y_{b2})$ and one of the middle control point of the right polygon (x_{c1}, y_{c1}), and only the *x* coordinate of the other control point (x_{c2}) of the right polygon constitute the seven designs variables in this problem. The *y* coordinate of the middle control point of the right polygon is fixed at the same value as the *y* coordinate of the input point in order to maintain the symmetry in slope at the input point. Here, an important property of Bezier curves is used in that the Bezier curve is tangential at the end point to the line joining the end point and the middle control point adjacent to it. The optimization problem in seven variables and eight constraints is stated below.

$$\begin{aligned}
&\min: -MSE(x_{b1}, y_{b1}, x_{b2}, y_{b2}, x_{c1}, y_{c1}, x_{c2}) \\
&s.t. \\
&g_1 = \sum_{i=1}^{NELEM} L_i - L_0 \leq 0 \\
&g_2 = y_{c1} - k_a x_{c1} \leq 0 \\
&g_3 = y_{c2} - k_a x_{c2} \leq 0 \\
&g_4 = l.a.c.1; \\
&g_5 = l.a.c.2; \\
&g_6 = x_{c1} - x^{LB} \leq 0 \\
&g_7 = x_{c2} - x^{UB} \leq 0 \\
&g_8 = x^{LB} - x_{c2} \leq 0
\end{aligned} \quad (14)$$

and equilibrium equations with boundary conditions.

where g_1 is the length constraint; g_2 and g_3 are geometric space constraints to prevent intersection of the two segments where k_a is the slope of the line that bounds the second segment to the right of the line joining the fixed point and the point where the two segments join; g_4 and g_5 are loop-avoidance constraints; and $g_6 - g_9$ are bounds on the variables to restrict the design to the prescribed

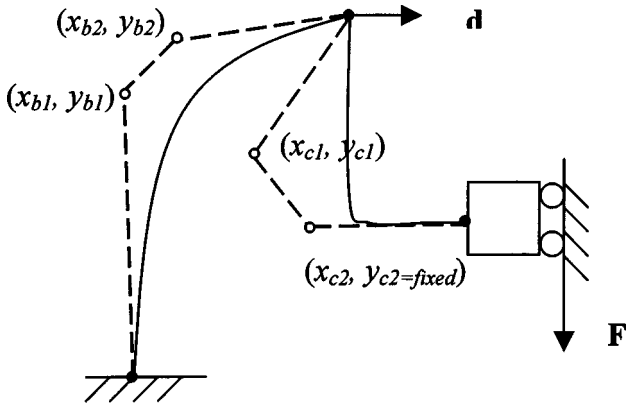

Fig. 8 Shape optimization problem specifications for the gripper

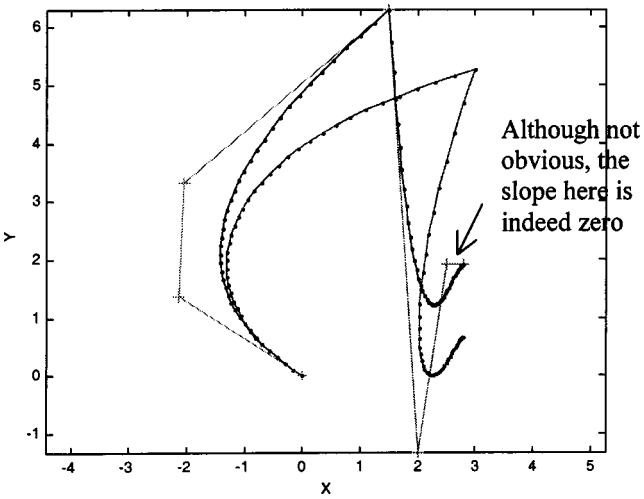

Fig. 9 Optimum solution and its deformed profile for the gripper

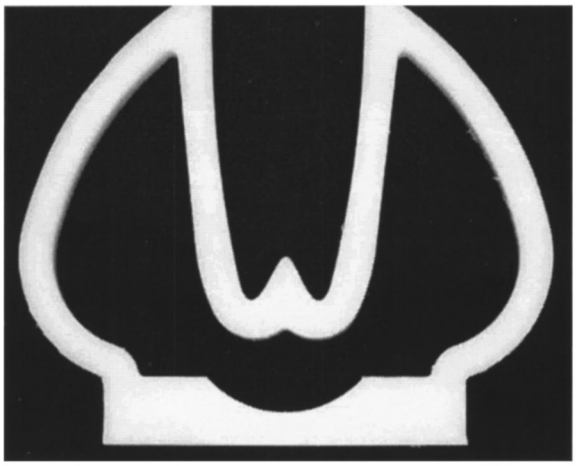

Fig. 11 Polyethylene prototype of the shape-optimized compliant gripper

region. Other parameters considered were: cross-sectional area area$=A=6.25e-2$ in^2; thickness$=t=2.5e-1$ in; moment of inertia$=In=3.2552e-04$ in^4; Young's modulus of material$=E=2.9e+05$ psi; and applied input force$=F=5$ lb.

For the initial guess of $[-1.0, 2.0, -2.0, 4.0, 1.0, 3.0, 2.0]$, the optimum solution shown in Fig. 9 was obtained. It should be noted that, the slope of the right end of the segments ending on the axis of symmetry is indeed is zero at that point although it is not obvious from the figure. This is because the curve starts here as a horizontal line (if we zoom in, it can be seen clearly), dips down and then moves up. The initial guess was chosen to be close to the shape of the gripper shown in Fig. 4(*a*). The optimum solution was found to be $[-2.1307, 1.3632, -2.0413, 3.3225, 2.0000, -1.3368, 2.500]$. The objective function history during the iterative process is shown in Fig. 10. The history shows both feasible and infeasible designs that occurred during the search. It can be seen that the objective function was decreased from -0.9 to -1.5, which is a 67% improvement over the original design. The fabricated polyethylene prototype is shown in Fig. 11.

5.2 Example 2: Crimping Tool. The skeletal model of the top symmetric half of a crimping tool is shown in Fig. 12. This is an equivalent topology obtained by kinematically interpreting a topology optimization solution. This example is used in many papers in the literature. Here, only the essential topology and the identified compliant segments are taken. In this design, there are two segments to be optimized. The third straight-line segment is not optimized. Its end points on the two curved segments are chosen at fixed values of the parameter t in the respective Bezier curves. There are eight design variables in this example. The seven variables are similar to the ones in the last example. An eighth one (y_{b0}) is added to vary the y coordinate of the fixed point A. The optimization problem statement is shown in Eq. (15). The explanation of all the constraints is the same as in the previous example.

$$\begin{aligned}
&\min: -MSE(x_{b1}, y_{b1}, x_{b2}, y_{b2}, x_{c1}, y_{c1}, y_{c2}, y_{b0}) \\
&s.t. \\
&g_1 = \sum_{i=1}^{NELEM} L_i - L_0 \leq 0 \\
&g_2 = y_{c1} - k_b x_{c1} \leq 0 \\
&g_3 = y_{c2} - k_b x_{c2} \leq 0 \\
&g_4 = lac1; \\
&g_5 = lac2; \\
&g_6 = y_1^{LB} - y_{c1} \leq 0 \\
&g_7 = y_2^{LB} - y_{c2} \leq 0
\end{aligned} \tag{15}$$

and equilibrium equations with boundary conditions.

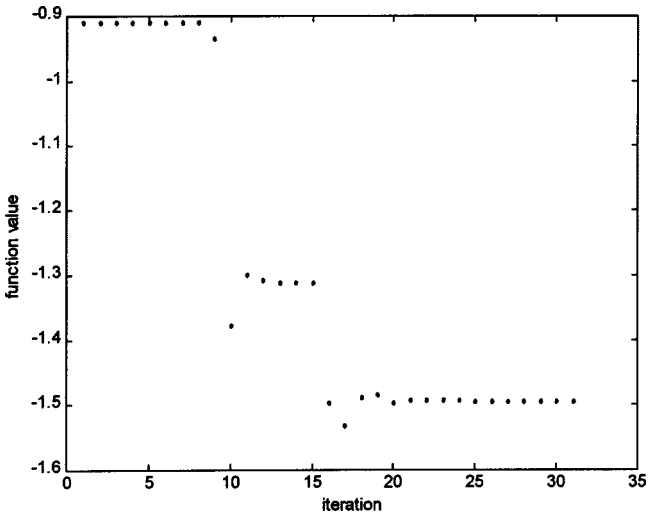

Fig. 10 Iteration history for the shape optimization of the gripper

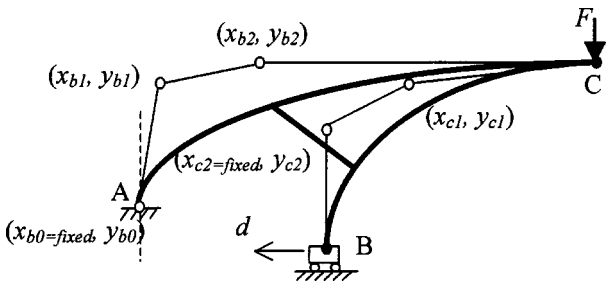

Fig. 12 Shape optimization problem specifications for the crimper

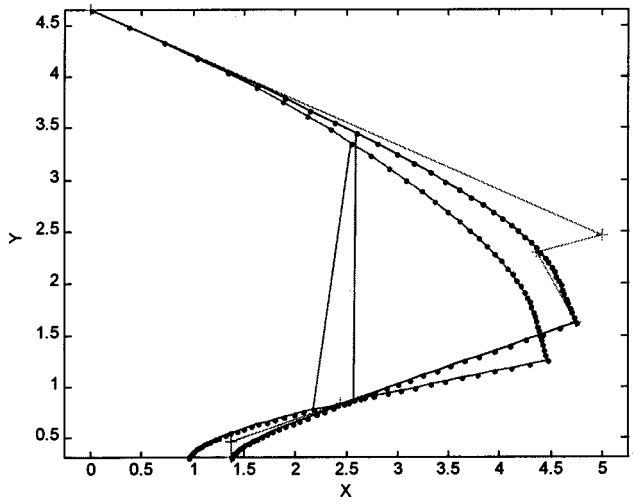

Fig. 13 Shape-optimized crimper and its deformed profile

The remaining data for this example was as follows: cross-sectional area $=A=6.25e-2$ in^2; thickness $=t=5e-1$ in; moment of inertia $=In=3.2552e-4$ in^4; Young's modulus of material $=E=2.9e+5$ lb/in^2; applied input force $=F=5$ lb. The initial guess was chosen such that the shape resembles that of an existing topology-optimized crimping tool. With the initial guess of $[-4.0593, 2.3791, -1.7885, 5.000, 2,1.9, 2.2, 1]$, an optimum solution was found to be: $=[5.0000, 2.4652, 4.3608, 2.2941, 2.4400, 0.8347, 0.4704, 4.6503]$. Figure 13 shows the optimum solution and its deformed profile. The objective function decreased from -0.025 of the initial design to -0.4 in the optimized design, which is a significant improvement. Fabricated polyethylene prototype is shown in Figs. 14(*a*) and 14(*b*) in its original and deformed configurations respectively.

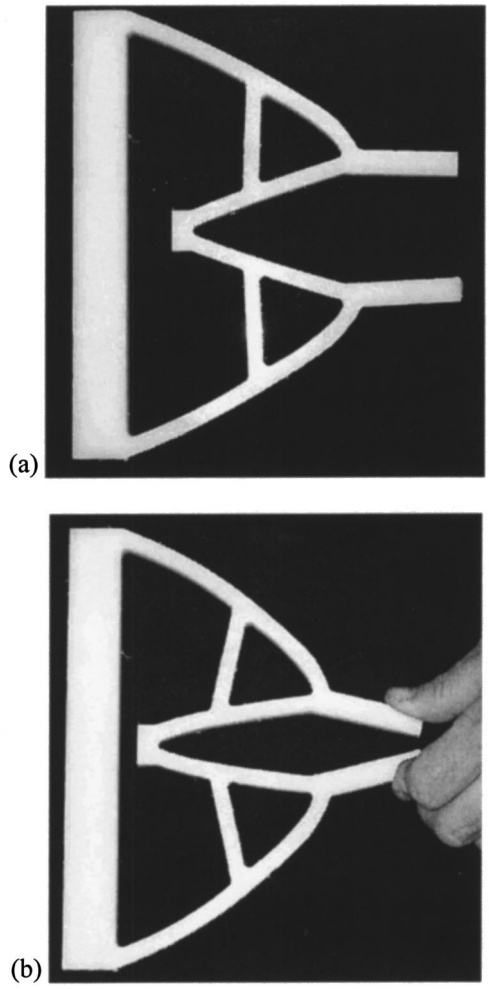

Fig. 14 Polyethylene prototype of the optimized crimping tool (*a*) undeformed (*b*) deformed under actuation

Conclusions

Although topology optimization methods developed for compliant mechanisms generate shape at the same time, there are some limitations to the generated shapes. This is true for both beam element-based ground structure as well as continuum element-based design parameterizations. In this paper, optimization of shapes of the compliant segments in a given topology is considered as a second-stage design. Systematic procedure for shape optimization including practical constraints and sensitivity analysis is presented. The width of the skeletal structure of the mechanism is held fixed but could be varied as well. Cubic Bezier curves were chosen to vary the shape as freeform curves because of their many attractive properties for shape optimization. The two examples presented indicate that substantial improvement can be achieved with shape optimization. The shape optimization has practical utility to further improve the compliant mechanism designs obtained with topology optimization or by other means.

Acknowledgments

This research was funded in part by the National Science Foundation grant (#DMR-90-00417). This support is gratefully acknowledged.

References

[1] Howell, L. L., and Midha, A., 1994, ''A Method for the Design of Compliant Mechanisms With Small-Length Flexural Pivots,'' ASME J. Mech. Des., **116**, pp. 280–290.
[2] Ananthasuresh, G. K., and Kota, S., 1995, ''Designing Compliant Mechanisms,'' Mech. Eng. (Am. Soc.. Mech. Eng.) **117**, (11), November, pp. 93–96.
[3] Moulton, T., and Ananthasuresh, G. K., 2001, ''Micromechanical Devices With Embedded Electro-Thermal-Compliant Actuation,'' Sens. Actuators A, **90**, pp. 38–48.
[4] Towfigh, K., 1969, ''The Four-Bar Linkage as an Adjustment Mechanism.'' *Oklahoma State University Applied Mechanism Conference*, July 31–Aug 1, Tulsa, Oklahoma, pp. 27.1–27.4.
[5] Byers, F. K., and Midha, A., 1991, ''Design of a Compliant Gripper Mechanism,'' *Proceedings of the 2nd National Applied Mechanisms & Robotics Conference*, Cincinnati, Ohio, pp. XC.1-1–XC.1-12.
[6] Crane, N. B., Howell, L. L., and Weight, B. L., 2000, ''Design and Testing of a Compliant Floating-Opposing-Arm (FOA) Centrifugal Clutch,'' *Proceedings of the 2000 ASME Design Engineering Technical Conferences*, DETC2000/MECH-14451.
[7] Ananthasuresh, G. K., and Saggere, L., 1994, ''Compliant Stapler,'' University of Michigan Mechanical Engineering and Applied Mechanics Technical Report, #UM-MEAM-95-20.
[8] Bar-Avi, P., and Benaroya, H., 1997, *Nonlinear Dynamics of Compliant Offshore Structures*, Advances in Engineering series, Swets & Zeitlinger, June.
[9] Saggere, L., and Kota, S., 1999, ''Static Shape Control of Smart Structures Using Compliant Mechanisms,'' AIAA J., **37**(5), pp. 572–578.
[10] Kota, S., Ananthasuresh, G. K., Crary, S. B., and Wise, K. D., 1994, ''Design and Fabrication of Microelectromechanical Systems,'' ASME J. Mech. Des., **116**, (4), March, pp. 1081–1088.
[11] Frecker, M., 2001, ''Design of Multifunctional Compliant Mechanisms for Minimally Invasive Surgery: Preliminary Results,'' paper #DAC-21055, 2001 ASME Design Automation Conference, Pittsburgh, PA, Sep. 9–12.
[12] Howell, L. L., 1993, ''A Generalized Loop-Closure Theory for the Analysis and Synthesis of Compliant Mechanisms,'' Ph.D. Thesis, Purdue University, West Lafayette, Indiana.
[13] Howell, L. L., and Midha, A., 1996, ''A Loop-Closure Theory for the Analysis and Synthesis of Compliant Mechanisms,'' ASME J. Mech. Des., **118**, pp. 121–125.
[14] Ananthasuresh, G. K., Kota, S., and Kikuchi, N., 1994, ''Strategies for Systematic Synthesis of Compliant MEMS,'' *Proceedings of the 1994 ASME Winter Annual Meeting*, Nov., Chicago, IL, pp. 677–686.
[15] Bendsoe, M. P., and Kikuchi, N., 1998, ''Generating Optimal Topologies in

Structural Design Using a Homogenization Method,'' Comput. Methods Appl. Mech. Eng., **71**, pp. 197–224.
[16] Zhou, M., and Rozvany, G. I. N., 1991, ''The COC Algorithm. 2. Topological, Geometrical and Generalized Shape Optimization,'' Comput. Methods Appl. Mech. Eng., **89**(1–3), pp. 309–336.
[17] Sigmund, O., 1997, ''On the Design of Compliant Mechanisms Using Topology Optimization,'' Mech. Struct. Mach., **25**(4), pp. 495–526.
[18] Nishiwaki, S., Frecker, M., Min, S., and Kikuchi, N., ''Topology Optimization of Compliant Mechanisms Using the Homogenization Method,'' Int. J. Numer. Methods Eng., **42**, pp. 535–559.
[19] Frecker, M. I., Anathasuresh, G. K., Nishiwaki, N., Kikuchi, N., and Kota, S., 1997, ''Topological Synthesis of Compliant Mechanisms Using Multi-Criteria Optimization,'' ASME J. Mech. Des., 238–245.
[20] Saxena, A., and Ananthasuresh, G. K., 2000, ''On an Optimal Property of Compliant Mechanisms,'' Structural and Multidisciplinary Optimization, **19**(1), pp. 36–49.
[21] Pedersen, C. B. W., Buhl, T., and Sigmund, O., 2001, ''Topology Synthesis of Large-Displacement Compliant Mechanisms,'' Int. J. Numer. Methods Eng., **50**, pp. 2683–2705.
[22] Topping, B. H. V., 1983, ''Shape Optimization of Skeletal Structures: A Review,'' J. Struct. Div. ASCE, **109**(8), pp. 1933–1951.
[23] Haftka, R. T., and Grandhi, R. V., 1986, ''Structural Shape Optimization—A Survey,'' Comput. Methods Appl. Mech. Eng., **57**, pp. 91–106.
[24] Phan, A.-V., and Phan, T.-N., 1999, ''A Structural Shape Optimization System Using the Two-dimensional Boundary Contour Method,'' Arch. Appl. Mech. **69**, pp. 481–489.
[25] Shi, X., and Mukherjee, S., 1999, ''Shape Optimization in Three-dimensional Linear Elasticity by the Boundary Contour Method,'' Eng. Anal. Boundary Elem. **23**, pp. 627–637.
[26] Sharatchandra, M. C., Sen, M., and Mohamed, G., 1998, ''New Approach to Constrained Shape Optimization Using Genetic Algorithms,'' AIAA J., **36**, (1), January.
[27] Annicchiarico, W., and Cerrolaza, M., 1999, ''Finite Elements, Genetic Algorithms and β-splines: A Combined Technique for Shape Optimization,'' Finite Elem. Anal. Design, **33**, pp. 125–141.
[28] Zienkiewicz, O. C., and Campbell, J. S., 1973, ''Shape Optimization and Sequential Linear Programming,'' R. H. Gallagher and O. C. Zienkiewicz, eds., *Optimum Syructural Design*, Wiley, New York, pp. 109–126.
[29] Yang, R. J., Dewhirst, D. L., Allison, J. E., and Lee, A., 1992, ''Shape Optimization of Connecting Rod Pin End Using a Generic Model,'' Finite Elem. Anal. Design, **11**, pp. 257–264.
[30] Tortorelli, D. A., Tomasko, J. A., Morthland, T. E., and Dantzig, J. A., 1994, ''Optimal Designs of Non-linear Parabolic Systems-Part II: Variable Spatial Domain With Applications to Casting Optimization,'' Comput. Methods Appl. Mech. Eng., **113**, pp. 157–172.
[31] Hetrick, J. A., and Kota, S., 1999, ''An Energy Formulation for Parametric Size and Shape Optimization of Compliant Mechanisms,'' ASME J. Mech. Des., **121**, pp. 229–234.
[32] Xu, D., 2000, ''Skeletal Shape Optimization of Compliant Mechanisms,'' *Masters thesis*, University of Pennsylvania.
[33] Yamaguchi, Fujio, 1988, *Curves and Surfaces in Computer Aided Geometric Design*, Springer, New York.
[34] Saxena, A., and Ananthasuresh, G. K., 2002, ''A Computational Approach to the Number Synthesis of Linkages,'' to appear in ASME J. Mech. Des., .
[35] Haftka, R., and Gurdal, Z., 1989, *Elements of Structural Optimization*, Kluwer Academic Publishers, Boston.